HIGH-RATE AND HIGH-ENERGY GAMMA-RAY SPECTROSCOPY USING CHARGE TRAPPING AND BALLISTIC DEFICIT CORRECTION CIRCUITS

M. L. Simpson, T. W. Raudorf, T. J. Paulus, R. C. Trammell
EG&G ORTEC
100 Midland Road
Oak Ridge, TN 37830, U.S.A.

Abstract

A study of the resolution of large, coaxial, reverse electrode, HPGe detectors was performed over the energy range from 100 keV to 10 MeV and triangular amplifier shaping times from 0.5 μs to 6 μs. Resolutions were calculated using an approach based on the Trammell-Walter equation [3]. The effect of ballistic deficit was included in the calculations by the introduction of a term, defined here as the "ballistic efficiency," to the Trammell-Walter equation. Experimental data were collected over an energy range from 122 keV to 2.6 MeV on three detectors with relative efficiencies of 76%, 56%, and 29%. These data were obtained using three instruments: A triangular shaping amplifier; a triangular shaping amplifier with charge trapping and ballistic deficit correction; and a gated integrator. Also, data were collected using a gated integrator with charge trapping correction on the detector with 76% relative efficiency. For these three detectors, the data indicate that the triangular shaping amplifier with charge trapping and ballistic deficit correction offered better resolution than a gated integrator for shaping times ≥2 μs, while the gated integrator produced better resolution for shaping times ≤1 μs. The data also show the added importance of charge trapping correction at high energies. For example, the detector with a relative efficiency of 29% had an uncorrected resolution of 1.98 keV with a 6 μs shaping time and at an energy of 1.33 MeV. However, at 10 MeV, the uncorrected resolution was predicted to be 7.3 keV, while an extrapolation of the data predicts a corrected resolution of 5.6 keV.

I. INTRODUCTION

Large, reverse electrode, coaxial, HPGe detectors are the detectors of choice in many experiments because of their high efficiency and high resistance to radiation damage. Due to their size, however, these detectors are more susceptible to peak broadening induced by charge trapping and ballistic deficit. Since ballistic deficit is inversely proportional to the square of the peaking time of the shaping amplifier [1], and charge trapping and ballistic deficit are proportional to energy [1], [2], the resolution degradation due to these phenomenon could dominate the line shapes in high-rate and high-energy spectroscopy. To compensate for the peak broadening mentioned above, a gated integrator or a ballistic deficit [1], or charge trapping correction circuit [2] can be employed. Ballistic deficit and charge trapping correction circuits are very similar, and in this work will be referred to collectively as resolution enhancement circuits.

Two charge trapping mechanisms may cause peak broadening, which will be defined here as deep-level and shallow-level trapping. A charge carrier that is captured by a deep-level trap will not be released quickly compared to the pulse processing time, while a carrier captured by a shallow-level trap will be released in a time shorter than the pulse processing time. Peak broadening induced by shallow-level charge trapping can be reduced by the use of a gated integrator, while only resolution enhancement circuits have been shown to be effective in correcting for deep-level trapping. In many cases, a detector that exhibits charge trapping will contain both shallow-level and deep-level traps.

Both the gated integrator and resolution enhancement circuits correct for ballistic deficit, but use distinctly different methods. The gated integrator integrates the voltage waveform from a pre-filter (usually semi-Gaussian). The output signal from the gated integrator is a function of the amount of charge produced by the detector, but does not depend upon the charge collection time if the charge collection time is shorter than the flat-top region of the gated integrator weighting function. A resolution enhancement circuit, however, adds a correction to the output of a spectroscopy amplifier that is a function of the charge collection time. Each method has advantages and disadvantages, and the best instrument to use for a particular application depends upon throughput requirements, energy range of interest, and both the densities and ratio of densities of shallow-level and deep-level traps.

Line shape calculations were performed over the energy range from 100 keV to 10 MeV for shaping times from 0.5 to 6 μs. Electronic noise, charge production statistics, majority carrier charge trapping, and ballistic deficit were accounted for in these calculations using an approach based on the Trammell-Walter equation [3]. Experimental results were obtained over the energy range from 122 keV to 2.6 MeV, with reverse electrode detectors having relative efficiencies of 76%, 56%, and 29% using a gated integrator and a triangular shaping amplifier with and without a resolution enhancement circuit. In addition, the detector having 76% relative efficiency was measured using a gated integrator to correct for ballistic deficit and shallow-level charge trapping, while a resolution enhancement circuit was used to correct the gated integrator output for deep-level charge trapping.

II. LINE SHAPE CALCULATIONS

The theory developed in this section describes the line shapes of spectral peaks produced by large reverse electrode (n-type) coaxial detectors. Ballistic deficit effects and majority carrier (electron) trapping are taken into account in addition to the broadening due to charge production statistics and electronic noise. True coaxial geometry (rather than the closed-end configuration favored by most manufacturers) and uniform gamma-ray irradiation are assumed. Also, the broadening due to trapping is considered to arise entirely from majority carrier (electron) traps with no minority (hole) carrier trapping occurring. Reverse electrode coaxial detectors generally exhibit a larger concentration of trapping centers at the detector periphery than at the inner region. This type of profile is modeled here by a trap distribution exponentially decreasing from the outer radius toward the center. The above considerations approximate the experimental case fairly well and facilitate the line shape computation.

The starting expression for the calculation is the Trammell-Walter equation [3] modified to account for ballistic deficit,

$$\frac{dN(E)}{dE} = \frac{1}{\sqrt{2\pi}} \int_{r_1}^{r_2} \frac{F(r)}{\sigma(r)} \exp\left[-\tfrac{1}{2}\left(\frac{E - \eta(r)\gamma(r,t_p)E_0}{\sigma(r)} \right)^2\right] dr, \quad (1)$$

where

E_0 = the actual gamma-ray energy,

E = the energy at which the expression is evaluated,

r_1 = the detector inner radius,

r_2 = the detector outer radius,

$dN(E)/dE$ = the rate of change with energy, at energy E, of the fraction of total events occurring and hence gives a value for one point on a complete line shape curve (Experimentally, $dN(E)/dE$ is proportional to the number of counts in an MCA channel),

$F(r)$ = the geometrical weighting factor for coaxial geometry,

$\sigma(r)$ = the standard deviation in pulse height,

$\eta(r)$ = the charge collection efficiency,

$\gamma(r,t_p)$ = the ballistic efficiency and accounts for the effect of ballistic deficit by allowing E_0 apparently to depend on radius, r, and peaking time t_p.

Each of these quantities will now be discussed in turn. F(r) is the geometrical weighting factor for coaxial detectors and is given by [4].

$$F(r) = 2r/(r_2^2 - r_1^2) \quad . \quad (2)$$

The standard deviation, $\sigma(r)$, may be expressed [5] as

$$\sigma(r) = [\sigma_F^2 + \sigma_N^2 + \sigma_T^2(r)]^{1/2} \quad , \quad (3)$$

where σ_F is the broadening due to charge production statistics, σ_N is the contribution of electronic noise, and $\sigma_T(r)$ is the broadening due to trapping.

$$\sigma_T(r) = \{\epsilon K E_0[1 - \eta(r)]\}^{1/2} \quad , \quad (4)$$

where ϵ is the average energy required to create an electron hole pair. K is an empirical constant determined by Raudorf and Pehl [5] to be ≈340.

The charge collection efficiency, $\eta(r)$, for the case where there is no hole trapping and for constant λ where λ is the mean free drift length for electrons is given by [5].

$$\eta(r) = [1/(\ln r_2/r_1)]$$

$$\{\ln (r_2/r) - e^{-r/\lambda}[\ln (r_1/r) - [(1/\lambda)(r-r_1)] - (1/4\lambda^2)(r^2-r_1^2)]\} \quad (5)$$

However, in general, λ is not constant with radius since it is a function of electric field, E. Following Raudorf and Pehl [5], λ is given by

$$\lambda = \frac{v_{drift}}{\sigma_e \langle v \rangle n_t(r)} \quad , \quad (6)$$

where v_{drift} is the electron drift velocity. V_{drift} may be represented empirically by

$$V_{drift} = \mu_0 E \,/\, \{[1 + (E/E_0)^{\beta}]^{1/\beta}\} \quad , \quad (7)$$

where μ_0 is the low field electron mobility and E_0 and ß are constants. For electrons in germanium at 80K, ß = 1.32 and E_0 = 275 V/cm. These values result in a reasonable approximation to the field dependent drift velocity according to Raudorf and Pehl. There is no simple analytical expression for <v>, the thermal velocity, either. Raudorf and Pehl used the following empirical expression for both electrons and holes

$$\langle v \rangle = \{[(3.2 \times 10^{-12})/m^*][(a + bE) - c \exp(-Ed)]\}^{1/2} , \quad (8)$$

where m* is the effective mass (g) and $a = 1.5 \times 10^{-2}$ eV, $b = 6.47 \times 10^{-6}$ eV, $c = 5.0 \times 10^{-3}$, and $d = 6.0 \times 10^{-3}$ cm/V. The electric field in the case of true coaxial geometry is given by

$$E = \tfrac{1}{2}(\rho/\epsilon_k)r - \{[V + \tfrac{1}{4}(\rho/\epsilon_k)(r_2^2 - r_1^2)] / [r \ln (r_2/r_1)]\}, \quad (9)$$

where ρ is the space charge density in the depleted region of the detector, ϵ_k is the dielectric constant of germanium, and V is the applied bias (V $\geq$ the depletion voltage). The electron trap cross section, σ_e, is represented by an expression of the form

$$\sigma_e = \sigma_{eo} / E^x \quad , \quad (10)$$

where σ_{eo} is the zero field cross section and x is a power factor of E. Both σ_{eo} and x are considered fitting parameters of the calculation. In practice, for the case of neutron damage created hole traps $x \approx 1.0$. For the case of electron traps in n-type coaxials $1.0 \leq x \leq 2.0$ with $x \approx 1.5$ being satisfactory in most cases. $n_t(r)$ is the trap density and, as discussed at the beginning of this section, is considered to be an exponential function of radius of the form

$$n_t = n_{to}\exp(-r/L) \quad , \quad (11)$$

where n_{to} is the trap density at r_2 and L is a characteristic length. Both n_{to} and L may be considered as fitting parameters of the calculation unless the actual trap distribution is known.

Every quantity in equation (6) is either directly r dependent or r dependent via the dependence of E on r. As pointed out by Raudorf and Pehl, it is technically incorrect to calculate $\eta(r)$ as in equation (5) by assuming an r independent λ. However, the parameters in equation (6) tend to vary in a manner that the total dependence of λ on r is not extreme. Raudorf and Pehl as an approximation substituted equation (6) directly into equation (5) and found it to be acceptable. A better approximation, however, is to calculate an average value of λ for each r in equation (5) or, more appropriately since it is λ^{-1} that is used in the computation,

$$(1/\lambda)_{av} = [1/(r_1 - r)] \int_{r'}^{r_1} (1/\lambda)\, dr' \quad . \quad (12)$$

Hence for each value of $\eta(r)$ the value of λ_{av}^{-1} calculated numerically from equation (12) was used.

The ballistic efficiency, $\gamma(r,t_p)$, was determined as follows: The preamplifier pulse shapes calculated by Raudorf, et al. [4] were expressed as piece-wise linear functions and used as inputs to a PSpice [6] model of a triangular shaping spectroscopy amplifier. PSpice was used to calculate the amplitude (V_0) of the resulting amplifier output pulses. The ballistic deficit was

$$BD = V_0|_{tr=0} - V_0 \quad , \quad (13)$$

where $V_0|_{tr=0}$ was the amplitude of the spectroscopy amplifier output for an input signal with zero rise time ($t_r=0$). Equation (13) was plotted versus the interaction radius and was expressed as a piece-wise linear function, f(r). The t_p^{-2} dependence of ballistic deficit was included [1], and equation (13) then becomes

$$BD(r,t_p) = \{K_1[V_0|_{tr=0} - V_0(r)]\} / t_p^2 \quad , \quad (14)$$

where K_1 is a normalizing constant. The function of equation (14) is similar to the result of Goulding and Landis [1], but allows for more accurate calculations, especially at short shaping times since actual preamplifier pulse shapes were used in the calculation. Finally, the ballistic efficiency is calculated as

$$\gamma(r,t_p) = 1 - \{[BD(r,t_p)] / V_0|_{tr=0}\} \quad . \quad (15)$$

The actual expression used in the calculation was

$$\gamma(r,t_p) = 1 - (1.2\{2.32\times10^{-2} - 4.97\times10^{-2}[(r-r_1)/(r_2-r_1)]\})/t_p^2$$

for $r_1 \leq r < 0.33(r_2 - r_1) + r_1$;

$$\gamma(r,t_p) = 1 - [1.2\,(6.99 \times 10^{-3})] / t_p^2 \quad , \quad (16)$$

for $0.33(r_2 - r_1) + r_1 \leq r < 0.48(r_2 - r_1) + r_1$;

and

$$\gamma(r,t_p) = 1 - (1.2\{4.53\times10^{-2}[(r-r_1)/(r_2-r_1)] - 1.47\times10^{-2}\}) / t_p^2$$

for $0.48(r_2 - r_1) + r_1 \leq r \leq r_2$.

Equation (1) was numerically integrated for different values of E to determine the complete line shape. In practice, after the given quantities of the detector-amplifier system were entered into the calculation, the adjustable parameters n_{to}, L, and σ_{eo} were chosen to give the best fit to the measured line shape at 1.33 MeV. Instead of varying values of L, however, it was found more convenient to specify the trap concentrations at r_2 (i.e., n_{to}) and r_1. L is then automatically determined. Once the best fit was achieved at 1.33 MeV, E_0 was varied to calculate the expected energy resolution for values in the range from 100 keV to 10 MeV.

III. INSTRUMENTAL CONSIDERATIONS

The main disadvantage of the gated integrator, poor low-frequency noise performance, is not a problem with resolution enhancement circuits. However, these circuits rely upon accurate time and amplitude measurements to compute their correction, and may introduce a new noise source. Consider the case of ballistic deficit correction, where a resolution enhancement circuit would compute [1]

$$V_c = K_g S t_d^2 \quad , \tag{17}$$

where V_c is the correction voltage, K_g is the correction gain, S is the peak amplitude signal from the spectroscopy amplifier, and t_d is the unipolar peak delay time as defined in reference [1]. The problem is to determine the standard deviation of V_c, σ_{vc}, for a given nominal value of S and t_d.

The mean and mean-squared value of V_c are given by

$$\overline{V_c} = K_g \overline{S}\, \overline{t_d^{\,2}} \tag{18a}$$

$$\overline{V_c^{\,2}} = K_g^2 \overline{S^2}\, \overline{t_d^{\,4}} \quad , \tag{18b}$$

where S and t_d are assumed to be statistically independent. Since $\overline{S^2} = \overline{S}^2 + \sigma_S^2$, equation (18b) can be written

$$\overline{V_c^{\,2}} = K_g^2[\overline{S}^2 + (\sigma_S)^2]\overline{t_d^{\,4}} \quad . \tag{19}$$

In a high-resolution system such as a germanium spectrometer, S » σ_S, and σ_S^2 can be dropped from equation (19). σ_{vc} can then be calculated as follows:

$$\begin{aligned} \sigma_{vc} &= (\overline{V_c^{\,2}} - \overline{V_c}^2)^{1/2} \\ &\approx K_g \overline{S}[\overline{t_d^{\,4}} - (\overline{t_d^{\,2}})^2]^{1/2} \\ &= K_g \overline{S}[\sigma(t_d^2)] \quad . \end{aligned} \tag{20}$$

By a straightforward, although tedious, calculation, σ_{td}^2 can be expressed as

$$\sigma(t_d^2) \approx 2\overline{t}_d \sigma_{td} \quad , \tag{21}$$

and

$$\sigma_{vc} \approx 2K_g \overline{S}\, \overline{t_d}\, \sigma_{td} \quad . \tag{22}$$

Practical values of K_g range from 5×10^{10} for moderate charge trapping correction, to 4×10^{11} or more for ballistic deficit correction at short shaping times A large detector would have unipolar peak delay times in the range of 200 ns, and a σ_{td} of about 1 to 2 ns. σ_{vc} then would range from 0.002% of S for charge trapping correction, to 0.03% of S for ballistic deficit correction at short shaping times. Thus, this noise source is negligible for the case of moderate charge trapping, but can be significant for ballistic deficit.

In addition to the above mentioned noise source, resolution enhancement circuits suffer from two non-ideal effects. Ballistic deficit is given by [1]

$$BD = E_0(t_d/t_p)^2 \quad , \tag{23}$$

where E_0 is the energy of the gamma ray and t_p is the peaking time of the spectroscopy amplifier. However, the correction for the ballistic deficit is calculated using the energy measured by the spectroscopy amplifier, which includes the ballistic deficit. Thus,

$$\begin{aligned} C &= [E_0 - E_0(t_d/t_p)^2](t_d/t_p)^2 \\ &= E_0(t_d/t_p)^2 - E_0(t_d/t_p)^4 \quad , \end{aligned} \tag{24}$$

where C is the correction. The first term on the right of equation (24) is the desired correction, while the second term on the right is an error term. This error is negligible at long shaping times, where $t_d \ll t_p$, but can be significant at shorter shaping times. For example, for t_p = 1.6 µs, t_d = 300 ns, and E_0 = 1332.5 keV, the error would be 1.64 keV. It may be possible to eliminate this error using the circuit shown in Fig. 1. This circuit sums the correction with the input signal and then recalculates the correction continuously. The same argument can be applied in the case of charge trapping correction, but would only be important for the case of severely radiation-damaged detectors.

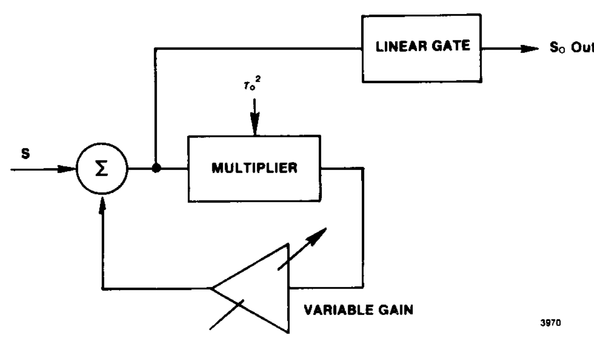

Fig. 1. Circuit to Compensate for Incomplete Correction of Ballistic Deficit. This circuit involves positive feedback, but the magnitude of the loop transmission is «1.

Equation (23) was derived assuming that the signals from the preamplifier were a linear function of time [1]. However, as shown by Raudorf, et al. [4], preamplifier signals generated by gamma rays which interact at a single point in the detector are not a linear function of time. The preamplifier signals generated by gamma rays which interact at multiple points in the detector can be treated as a linear superposition of single interaction point gamma rays. Figure 2 shows the ballistic deficit calculated by PSpice [6] using the preamplifier signals of Raudorf, et al. [4] minus the ballistic deficit calculated by equation (23) as a function of the normalized interaction radius. This figure illustrates that equation (23) is a very reasonable approximation at long shaping times. However, at short shaping times, the error in equation (23) is significant. Simpson, et al. [2] showed that the charge trapping correction circuit has a non-ideal feature similar to the one mentioned above for ballistic deficit correction. It is interesting to note that Fig. 2 predicts that interactions occurring at small radii will be under-corrected for the case of ballistic deficit, while Simpson, et al. showed that an over-correction will be calculated for interactions at small radii for the case of charge trapping correction.

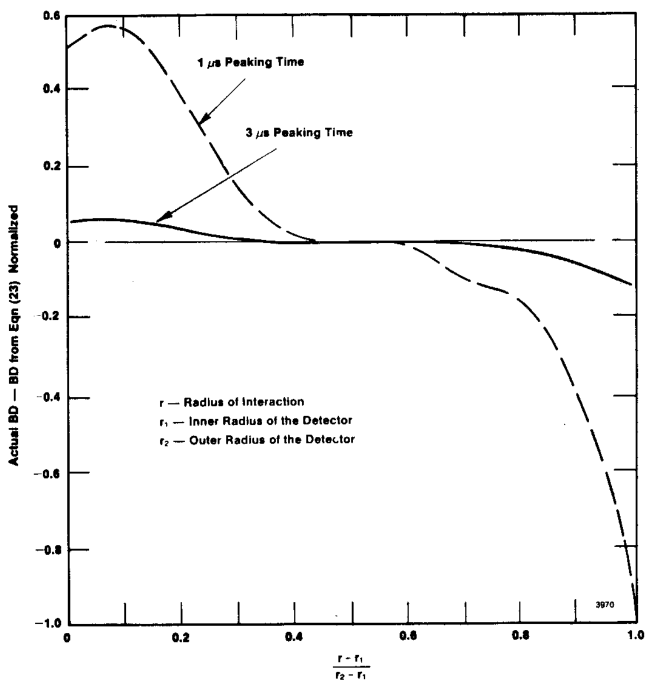

Fig. 2. Normalized Error in the Ballistic Deficit Correction as a Function of Interaction Radius for 1-μs Peaking Time and 3-μs Peaking Time.

The above discussion indicates that resolution-enhancement circuits will be superior to gated integrators when correcting for deep-level charge trapping at all shaping times, and when correcting for ballistic deficit and shallow-level charge trapping at moderate and long shaping times. The shaping times that form the boundary of superiority for the resolution enhancement circuits, however, must be determined experimentally.

IV. Experimental Results

Figure 3 depicts the resolution of three reverse electrode, coaxial, HPGe detectors having relative efficiencies of 76%, 56% and 29% as a function of the dead-time-per-pulse. The dead-time-per-pulse is the amount of dead time calculated using the Gedcke-Hale live time correction scheme [7] for one nonpiled-up event. The conversion time of the subsequent ADC is neglected here. For these detectors, Fig. 3 clearly shows that a resolution enhancement circuit is superior to the gated integrator for pulse dead times greater than 15 μs (this corresponds to triangular shaping with an ~1.5 μs shaping time), while the gated integrator is superior for pulse dead times less than 10 μs (which corresponds to ~1 μs shaping time triangular amplifier) at the 1.33-MeV line. Figure 3A also presents data taken with a gated integrator that employed a resolution-enhancement circuit to correct for charge trapping. This circuit offered the best resolution for pulse dead times less than 43 μs (~4.4 μs shaping time triangular amplifier) for this detector.

Figure 4 is the same as Fig. 3A, except these data were collected at the 2.6-MeV energy line. A comparison between Figs. 3A and 4 shows that at 2.6 MeV the crossover point between the uncorrected gated integrator and the corrected triangular shaping amplifier occurred at a shorter pulse dead time, but the corrected gated integrator offered the best resolution for all pulse dead times considered.

Figure 5 shows the resolution as a function of energy for the detectors of Fig. 3 at a 6 μs shaping time. The resolutions as a function of energy are also shown being calculated as described in Section II for the two limiting cases of total and zero correction for both ballistic deficit and charge trapping. The calculation for the case of zero correction in Fig. 5B was broken into two regions (break point at 1.17 MeV) to reflect an axial dependence of the detector trap distribution. The detector with 76% relative efficiency in Fig. 5A shows a significant amount of trapping even at 661.66 keV. Thus, as would be expected, a very large improvement in resolution could be realized at higher energies. For example, theoretically it is predicted that the resolution of the 76% efficient detector should be 9.3 keV at an energy of 10 MeV. However, extrapolation of the measured data suggests that the resolution of this detector would be 7 keV and 5.6 keV, respectively, for a corrected triangular shaping amplifier and a corrected gated integrator at 10 MeV. However, even though the detectors of Figs. 5B and 5C exhibited only moderate charge trapping, significant resolution improvements are possible. For example, in Fig. 5B the uncorrected resolution predicted by equation (1) at 10 MeV is 8 keV, while the extrapolation of the corrected

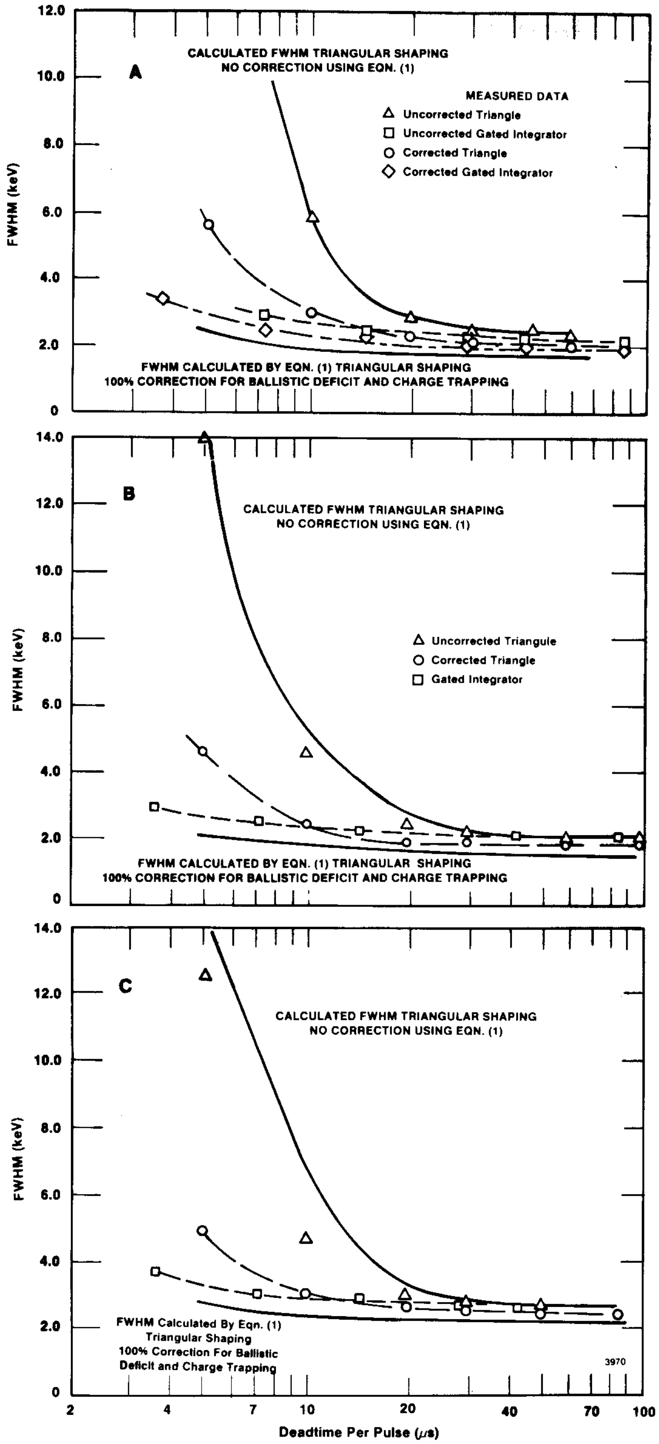

Fig. 3. Resolution vs Deadtime-per-Pulse for Detectors with Relative Efficiencies of (A) 76%, (B) 56%, and (C) 29%.

Parameters of Calculation for Figures

(A)

r_1 = 0.5 cm
r_2 = 3.6 cm
electronic noise = 0.85 keV
depletion voltage = −2200 V
operating bias = −3500 V
$n_{to}\sigma_{eo}$ = 40 cm^{-1}
$n_t|_{r1}\sigma_{eo}$ = 1.6 cm^{-1}

(B)

r_1 = 0.5 cm
r_2 = 3.30 cm
electronic noise = 0.63 keV
depletion voltage = −2200 V
operating bias = −3000 V
$n_{to}\sigma_{eo} = n_t|_{r1}\sigma_{eo}$ = 3.6 cm^{-1} 0.1 to 1.3 MeV
$n_{to}\sigma_{eo} = n_t|_{r1}\sigma_{eo}$ = 5.2 cm^{-1} 1.3 to 10 MeV

(C)

r_1 = 0.5 cm
r_2 = 2.9 cm
electronic noise = 0.60 keV
depletion voltage = −1500 V
operating bias = −3000 V
$n_{to}\sigma_{eo}$ = 56 cm^{-1} for E calculation
$n_t|_{r1}\sigma_{eo}$ = 1.4 cm^{-1}
$n_{to}\sigma_{eo}$ = 32 cm^{-1} for t_p calculation
$n_t|_{r1}\sigma_{eo}$ = 0.8 cm^{-1}

triangular shaping amplifier predicts a resolution of 6.7 keV. In Fig. 5C the predicted uncorrected resolution is 7.3 keV, while the predicted corrected resolution is 5.6 keV.

It should also be noted in Fig. 5A that the corrected triangular shaping amplifier provided better resolution than the corrected gated integrator at energies below 1.5 MeV, while the corrected gated integrator was superior at energies above 2.5 MeV. This can be explained as follows. At this long shaping time and at energies below 1.5 MeV, ballistic deficit is negligible, and electronic noise, charge generation fluctuations, and charge trapping are the dominant peak-broadening mechanisms. For the measurements made in this work, below 1.5 MeV the lower electronic noise of the corrected triangular shaping amplifier provided better resolution than the corrected gated integrator. However, at energies above 1.5 MeV, the electronic noise became a diminishing component of the energy resolution, and between 1.5 MeV and 2.5 MeV the corrected triangular shaping amplifier and corrected gated integrator offered essentially the same resolution. Above 2.5 MeV, ballistic

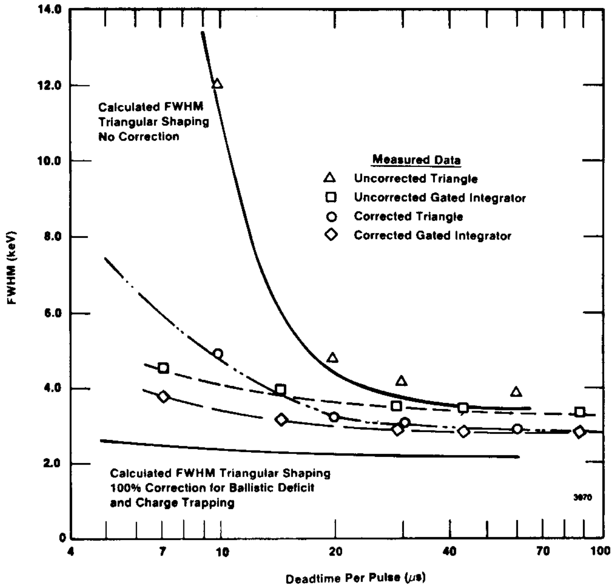

Fig. 4. **FWHM vs Deadtime-Per-Pulse at 2.61 MeV.**

deficit began to be an important component of the energy resolution. As discussed in the previous section, resolution enhancement circuits do not make a complete correction for ballistic deficit. Therefore, above 2.5 MeV, the corrected gated integrator was superior to the corrected triangular shaping amplifier. At shorter shaping times, ballistic deficit becomes important at lower energies and the corrected gated integrator would offer the better resolution at these lower energies when shorter shaping times are employed.

V. CONCLUSIONS

As Figs. 3, 4 and 5 illustrate, both the gated integrator and resolution enhancement circuits have energy/shaping time regimes where they are the better instrument. Since the gated integrator cannot correct for deep-level charge trapping, the resolution enhancement circuit will outperform the gated integrator at long shaping times. Conversely, since the resolution enhancement circuits do not completely correct for ballistic deficit, the gated integrator will be the better instrument at short shaping times. In between these two shaping time extremes, the instrument of choice is determined by the amount of deep-level charge trapping and the energy range of interest. However, the data from the preceding section suggest the following. At pulse dead times of 15 μs (~1.5 μs shaping time triangular amplifier) and above, a resolution enhancement circuit would usually be the instrument of choice, while the gated integrator should be used at pulse dead times below 10 μs (~1 μs shaping time triangular amplifier). At pulse dead times between 10 and

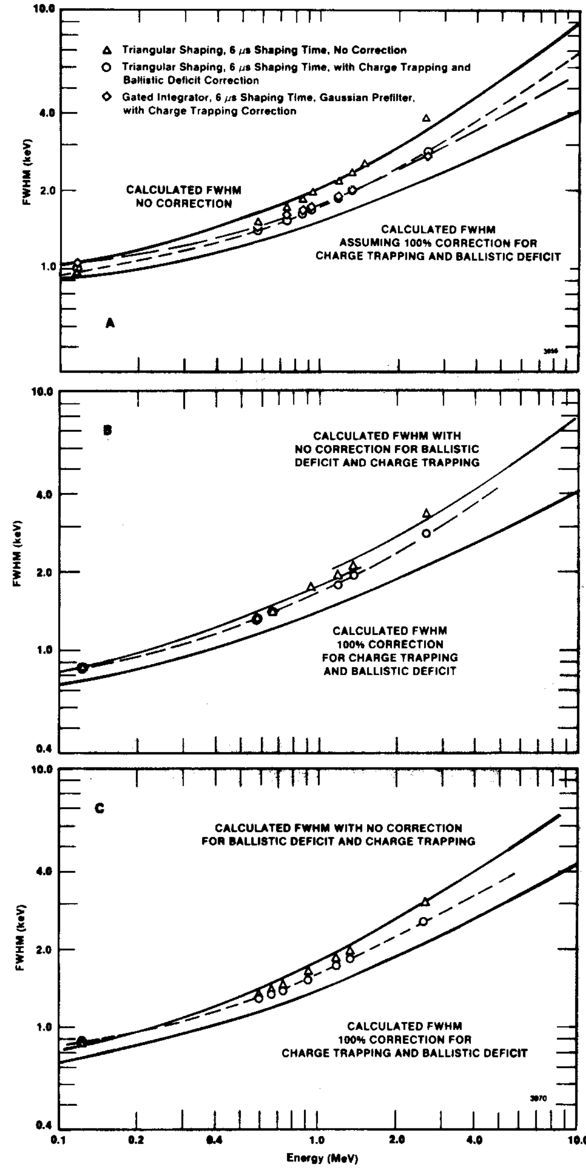

Fig. 5. **FWHM vs Energy at 6 μs Shaping Time.** Parameters of calculation are the same as for Fig. 3.

15 μs, the resolution offered by the two instruments would be nearly the same, with resolution enhancement circuits having the advantage if a great deal of deep-level charge trapping were present. However, the gated integrator would have an advantage with large detectors since the magnitude of the ballistic deficit would be larger.

Figures 3A, 4, and 5A suggest that a gated integrator with a resolution enhancement circuit could also be a useful circuit. However, more research is needed to map out the energy/shaping time regimes in which this instrument would be most appropriate.

Acknowledgements

The authors would like to acknowledge T. Becker for his many helpful suggestions and comments; L. Buker for her assistance in obtaining the radiation sources used in this work; J. Schall for producing the figures presented here; M. Apple for typing this manuscript; and B. Graham for editing and formatting the text.

References

[1] F. S. Goulding and D. A. Landis, *IEEE Trans. Nucl. Sci.*, NS-35, (1988) 119.

[2] M. L. Simpson, T. W. Raudorf, T. J. Paulus, and R. C. Trammell, *IEEE Trans. Nucl. Sci.*, NS-36, (1989) 260.

[3] R. C. Trammell and F. J. Walter, *Nucl. Instr. and Meth.*, 76 (1969) 317.

[4] T. W. Raudorf. T. J. Paulus, and M. O. Bedwell, *IEEE Trans. Nucl. Sci.*, NS-29, (1982) 764.

[5] T. W. Raudorf and R. H. Pehl, *Nucl. Instr. and Meth.*, A255 (1987) 538.

[6] P. W. Tuinenga, *SPICE, A Guide to Circuit Simulation and Analysis Using PSpice*. Englewood Cliffs, New Jersey: Prentice Hall, 1988.

[7] R. Jenkins, R. W. Gould, and D. Gedcke, *Quantitative X-ray Spectrometry*. New York: Marcel Dekker, Inc., 1981.

Printed in U.S.A. 3970 1089